CDF/ANAL/EXOTIC/PUBLIC/7307
Version 3.0

Search for the Wh Production Using High-p_T Isolated Like-Sign Dilepton Events in Run-II with 2.7 fb^{-1}

The CDF Collaboration
URL http://www-cdf.fnal.gov
(Dated: December 19, 2008)

We search for the neutral higgs production associated with the W boson using high-p_T isolated like-sign dilepton events in $p\bar{p}$ collisions at $\sqrt{s} = 1.96$ TeV. The data were collected with the CDF-II detector at the Fermilab Tevatron collider and correspond to an integrated luminosity of 2.7 fb^{-1}. The expected number of backgrounds is 188 $\pm$ 24 for the events with the first lepton p_T larger than 20 GeV/c and the 2nd lepton p_T larger than 6 GeV/c in the CDF central region, $|\eta| < 1.1$, while we observe 172 events in the data to find no significant disagreements. The expected number of signal events is 1.03 for the fermiophobic higgs of the mass 120 GeV/c^2 assuming the Standard Model cross section and 0.40 for the mass 160 GeV/c^2. The number of events for the Standard Model higgs is 0.14 and 0.38 for 120 GeV/c^2 and 160 GeV/c^2, respectively. We apply the Boosted Decision Tree technique for separating the backgrounds and signal events to improve the search sensitivity, then calculate limits in the Bayesian framework using the output distributions. We obtain the limits on $\sigma(p\bar{p} \rightarrow Wh) \times Br(h \rightarrow W^+W^-)$ of 1.80 pb for the higgs of 120 GeV/c^2 and 1.23 pb for 160 GeV/c^2 at the 95% confidence level.

Preliminary Results for Winter 2009 Conferences

I. INTRODUCTION

In the Standard Model, the higgs boson is introduced to explain the electroweak symmetry breaking and the origin of fermion masses. The direct search at the CERN e^+e^- collider (LEP2) presents a lower limit on the higgs boson mass of $m_h > 114.4$ GeV/c^2 at the 95% confidence level (C.L.). Indirect measurements, electroweak global fits, give an upper limit of 144 GeV/c^2 at the 95% C.L. which increases to 182 GeV/c^2 when the direct search is included [1].

Our physics objective is to search for the low-mass fermiophobic higgs and the high-mass Standard Model higgs boson using like-sign dilepton events produced by

$$qq' \to W^{\pm}h \to W^{\pm}W^*W^* \to \ell^{\pm}\ell^{\pm} + X.$$

The relevant higgs mass regions are above 110 GeV/c^2 for the fermiophobic higgs where the branching fraction of $h \to W^*W^*$ supersedes that of $h \to \gamma\gamma$, and above 160 GeV/c^2 for the Standard Model higgs where the branching fraction of $h \to b\bar{b}$ is overtaken by this channel.

The fermiophobic higgs boson has no coupling to the fermions. Existence of the fermiophobic higgs could be an indication that the origin of particle masses would be different for the bosons and the fermions. Such a particle can also arise as a CP-even scalar h^0 in the two higgs doublet model (2HDM) type I. The model has seven degrees of freedom: the five particle masses (h^0,H^0, A^0, $H^{\pm}$) and two angles (α, β). In the type I, the lightest CP-even scalar h^0 couples to a fermion proportionally to $\cos\alpha$, and the h^0 becomes a fermiophobic higgs when $\alpha = \pi/2$.

II. DATA SAMPLE & EVENT SELECTION

This analysis is based on the data with an integrated luminosity of 2.7 fb^{-1} collected with the CDF-II detector between March 2002 and April 2008. Detailed descriptions of the CDF-II detector can be found in [3]. The data are collected with inclusive lepton triggers that requires an electron with transverse energy (E_T) > 18 GeV or a muon with transverse momentum (p_T) > 18 GeV/c. Starting from the inclusive lepton datasets, we apply a number of event selection criteria to obtain a baseline dilepton sample. The events are required to have primary vertices within the region to ensure well-defined measurement of collisions by the detector and to pass a cosmic-ray veto. We select events at least one electron with $E_T > 20$ GeV and $p_T > 10$ GeV/c, or muon with $p_T > 20$ GeV/c, which is considered to be responsible for firing the triggers we have chosen, and at least one other electron with $E_T > 6$ GeV and $p_T >$ 6 GeV/c, or muon with $p_T > 6$ GeV/c, as the baseline dilepton selection. The leptons must be found in the central detector ($|\eta| < 1.1$) and within fiducial regions of the sub-detectors. They are also required to be isolated in terms of the calorimeter cone-isolation, with a cone size of $R = 0.4$, to be less than 2 GeV, where $R = \sqrt{(\Delta\eta)^2 + (\Delta\phi)^2}$ is the radius in the η-ϕ space, $\eta = -\ln(\tan\theta/2)$ is the pseudorapidity, the θ is the polar angle with respect to the proton beam direction, and ϕ is the azimuthal angle. The leptons must have a well-measured track, found both in the outer tracking chamber and the inner silicon detector, with the z coordinate and the impact parameter at the closest approach point to the beamline being consistent with coming from the primary vertex. We then apply a series of lepton identification cuts which impose various internal consistencies of information obtained from sub-detectors and require detector responses consistent with electrons or muons. If the electron is consistent with being due to a photon conversion as indicated by the presence of an additional nearby track, the electron is vetoed.

For the exactly two-lepton events passing our selection above, we explicitly require a cut to ensure that the two leptons are coming from the same vertex, and also apply a dilepton mass cut ($M_{\ell\ell} > 12$ GeV/c^2) and a Z-event veto. We finally require the like-sign charge combination to complete the event selection.

III. ACCEPTANCE AND EXPECTED EVENTS FOR SIGNAL

We get the signal acceptance 2.2-3.0% for higgs mass of 110-200 GeV/c^2 passing event selections, where the denominator is the number of $W^{\pm}h \to W^{\pm}W^*W^* \to$ at least 2-lepton events. The branching fraction corresponding to events with at least 2 leptons from triple Ws is about 0.12. The expected number of events are 0.08-0.10 for fermiophobic higgs, while 0.06-0.20 events for SM higgs. TABLE I shows the theoretical cross section and branching fraction ($h \to WW$) in each higgs mass to be used in the estimation of higgs acceptance and expected events. TABLE II shows the acceptance and expected events for signal events in each higgs mass, the uncertainties include MC statistics and uncertainties of MC scale factors.

IV. BACKGROUNDS

Although the like-sign requirement is quite effective to suppress QCD and known electroweak processes, we expect that fake-lepton backgrounds and residual photon-conversions still remain at a considerable level in the events of our signature. They are estimated by data-driven methods, while other backgrounds containing prompt real-leptons (physics backgrounds) are estimated by Monte Carlo (MC) data.

A. Physics Backgrounds

The physics backgrounds can be classified into reducible and irreducible backgrounds. The reducible backgrounds are Drell-Yan, WW, $t\bar{t}$, and W + (heavy-flavor hadrons), while irreducible backgrounds are WZ and WW. The reducible backgrounds are reduced by the isolation cut and like-sign requirement. Contributions of the irreducible backgrounds are small due to their small production cross sections, which are further suppressed by the Z-event veto. Since fake-leptons and residual photon-conversions are estimated separately using real data, we reject them found in the MC by looking at the generator-level information to avoid double counting.

B. Residual Photon-Conversion Background

The residual photon-conversion backgrounds arise from an electron originating from the photon conversion with an unobserved partner track due to its low momentum. We estimate the backgrounds by multiplying lepton + conversion events by residual photon-conversion rate (R_{res}). We define the rate by

$$R_{\mathrm{res}} = \frac{1-\varepsilon_{\mathrm{con}}}{\varepsilon_{\mathrm{con}}},$$

where $\varepsilon_{\mathrm{con}}$ is the conversion detection efficiency. The efficiency is measured by comparing the conversions found in the real data with conversion MC samples that are tuned to match with the sub-sample of real conversions in the high-p_T region of partner-tracks where the efficiency is well known. The residual conversion rate is parametrized by the parent photon p_T and is shown in FIG. 1.

C. Fake Lepton Background

The fake electron backgrounds are interactive $\pi^{\pm}$, overlap of π^0 and a track, and residual photon-conversions. The fake muon backgrounds are punch-through hadrons and decay-in-flight muons from $\pi^{\pm}$ and $K^{\pm}$. We also regard leptons from semileptonic decays of heavy-flavor hadron as one of fake lepton backgrounds. These background objects are common in generic QCD events. We estimate the backgrounds by multiplying lepton + isolated track events by the fake lepton rates derived from inclusive jet samples. The fake lepton rate (R_{fake}) is defined as a rate of leptons in the jet samples relative to isolated tracks with certain energy depositions especially in the hadron calorimeters. The p_T cut is 6 GeV/c in accordance with the lower p_T cut of our event selection. We reject W and Z events to find leptons in the jet samples to avoid prompt real-leptons from electroweak processes. The fake lepton rate is shown in FIG. 2. The fake electron rates go through corrections to subtract residual conversions in the jet samples because we estimate the amount of residual photon-conversion events separately as mentioned in the previous section.

D. Expected Backgrounds

We look at the consistency between the data and background expectations in 4 regions on a 2 dimensional plane of the 2nd lepton p_T (p_{T2}) versus the dilepton system p_T (p_{T12}):

- Region 1 : $p_{T12} < 15$ GeV/c and $p_{T2} \geq 20$ GeV/c
- Region 2 : $p_{T12} < 15$ GeV/c and $p_{T2} < 20$ GeV/c
- Region 3 : $p_{T12} \geq 15$ GeV/c and $p_{T2} < 20$ GeV/c
- Region 4 : $p_{T12} \geq 15$ GeV/c and $p_{T2} \geq 20$ GeV/c.

The numbers are shown in TABLE III. We see no significant discrepancies between the data and background expectations.

V. BOOSTED DECISION TREE

We employ a multivariate analysis based on the Boosted Decision Tree (BDT) technique [4] to get more search sensitivity. We train the BDT using fake leptons and residual photon-conversions, because they are the main background for our LS dilepton analysis. We perform the training in each higgs mass sample, independently, using 8 kinematic variables as the inputs to the BDT:

- 1st lepton $p_T(p_{T1})$
- 2nd lepton $p_T(p_{T2})$
- Dilepton system $p_T(p_{T12})$
- Missing E_T
- Dilepton mass
- MetSpec : $\not\!\!E_T$ if $\Delta\phi(\not\!\!E_T$, ℓ or jet) $> \pi/2$ or
  . : $\not\!\!E_T \sin(\Delta\phi(\not\!\!E_T$, ℓ or jet)) if $\Delta\phi(\not\!\!E_T$,ℓ or jet) $< \pi/2$
- H$_T$ (Sum of p_{T1}, p_{T2}, jets E_T ($E_T > 15$ GeV and $|\eta| < 2.0$), and Missing E_T)
- Number of Jets with $E_T > 15.0$ GeV

FIG 3 and 4 show the BDT input variables for LS dilepton events. After the BDT training, we make the data through the trained BDT. FIG 5 shows the BDT outputs for LS dilepton events from the BDT trained for the $M_h = 110$ and 160 GeV/c^2.

VI. SYSTEMATIC UNCERTAINTY

The systematic uncertainties are estimated for the normalization (rate) systematic and the shape of the BDT outputs. TABLE IV and V are summaries of the rate systematic uncertainties for signal and backgrounds. The sources of the shape uncertainties include the jet energy scale of the MC samples, the fake rates, and the residual photon-conversion ratios.

VII. RESULTS

We see no significant discrepancies between background expectations and the data in the BDT outputs. Using these output distributions, we set the 95% C.L. upper limits on the cross section times branching fraction $\sigma(p\bar{p} \to Wh) \times Br(h \to W^+W^-)$ with the Bayesian approach as 1.80 pb for the higgs of the mass 120 GeV/c^2 and 1.23 pb for 160 GeV/c^2. TABLE VI shows the limit for each higgs mass point from 110 GeV/c^2 to 200 GeV/c^2. We also obtain the ratios of the limit to the prediction for fermiophobic higgs and to prediction for the Standard Model (assuming the Standard Model production cross sections), which are shown in TABLE VII and VIII, respectively.

VIII. CONCLUSIONS

We searched for the neutral higgs production associated with the W boson using high-p_T like-sign dilepton events using the data corresponding to an integrated luminosity of 2.7 fb^{-1}. The expected number of backgrounds in the final sample was 188 $\pm$ 24, while the actual number of observed events was 172. The expected number of signal events was 1.03 for the fermiophobic higgs of the mass 120 GeV/c^2 assuming the Standard Model production cross section and 0.38 for the Standard Model higgs of 160 GeV/c^2. We employed the Boosted Decision Tree technique for separating backgrounds and signal events in the final sample, and found no significant disagreements in the output distributions. We obtained the upper limits on the production cross-section times the branching fraction for the higgs with masses in the region from 110 GeV/c^2 to 200 GeV/c^2. The expected limit was 1.24 pb for the 120 GeV/c^2 higgs and 0.98 pb for the 160 GeV/c^2 higgs, while the observed limits were 1.80 pb and 1.23 pb, respectively. The expected limit on the ratio to the theoretical prediction for the cross section was 8.8 for the fermiophobic higgs of the mass 120 GeV/c^2 and 20.1 for the Standard Model higgs of the mass 160 GeV/c^2, while the observed limits were 12.9 and 25.1, respectively.

TABLE I: Theoretical cross sections and branching fractions in ecah higgs mass.

Higgs Mass (GeV/c^2)	$\sigma(p\bar{p}\to Wh)$ (fb)	$B_F(h\to WW)$ (Fermiophobic higgs)	$B_F(h\to WW)$ (SM higgs)
110	216.0	0.87	0.04
120	159.0	0.88	0.12
130	119.0	0.88	0.27
140	90.2	0.89	0.47
150	68.9	0.90	0.68
160	53.1	0.97	0.92
170	41.3	0.98	0.97
180	32.4	0.94	0.94
190	25.5	0.94	0.94
200	20.3	0.94	0.94

TABLE II: Acceptance and expected number of events for signal passing baseline events selections. MC statistic and MC scale factor uncertainty are included.

Higgs Mass (GeV/c^2)	Acceptance (%)	Expected Events (Fermiophobic higgs)	Expected Events (SM higgs)
110	2.16 ± 0.08	1.318 ± 0.024	0.061 ± 0.001
120	2.27 ± 0.09	1.033 ± 0.018	0.141 ± 0.003
130	2.37 ± 0.09	0.808 ± 0.014	0.248 ± 0.004
140	2.48 ± 0.09	0.648 ± 0.011	0.342 ± 0.006
150	2.50 ± 0.09	0.504 ± 0.008	0.381 ± 0.006
160	2.39 ± 0.08	0.400 ± 0.006	0.380 ± 0.007
170	2.45 ± 0.08	0.323 ± 0.005	0.320 ± 0.005
180	2.57 ± 0.09	0.255 ± 0.004	0.255 ± 0.004
190	2.78 ± 0.09	0.217 ± 0.003	0.217 ± 0.003
200	2.91 ± 0.10	0.180 ± 0.003	0.180 ± 0.003

TABLE III: Background expectations and observed number of events for like-sign dilepton events.

	Regions				
	1	2	3	4	Total
Definition	$p_{T12} < 15$ GeV/c $p_{T2} \geq 20$ GeV/c	$p_{T12} < 15$ GeV/c $p_{T2} < 20$ GeV/c	$p_{T12} \geq 15$ GeV/c $p_{T2} < 20$ GeV/c	$p_{T12} \geq 15$ GeV/c $p_{T2} \geq 20$ GeV/c	
Fakes	0.76	36.3	130	1.6	169
Photon-conversions	0.79	0.3	14	1.0	16
Total	1.55±0.65	36.6±6.2	144±17	2.6±1.3	185±24
(Stat.)	±0.29	±2.0	±4	±0.4	±5
(Syst.)	±0.59	±5.8	±16	±1.2	±24
WZ	0.145	0.058	1.28	1.76	3.23
ZZ	0.025	0.019	0.31	0.28	0.64
Total MC	0.170±0.021	0.077±0.011	1.59±0.19	2.04±0.24	3.88±0.45
(Stat.)	±0.007	±0.005	±0.02	±0.02	±0.04
(Syst.)	±0.017	±0.008	±0.17	±0.21	±0.40
(Luminosity)	±0.010	±0.005	±0.10	±0.12	±0.22
Total expected	1.71±0.65	36.6±6.2	145±17	4.7±1.3	188±24
Data	3	26	137	6	172

TABLE IV: Rate systematic uncertainty (%) for signal.

Mass (GeV/c^2)	110	120	130	140	150	160	170	180	190	200
MC statistics	1.01	0.98	0.96	0.94	0.93	0.96	0.94	0.92	0.88	0.86
MC scale factors	1.52	1.55	1.49	1.39	1.39	1.25	1.24	1.18	1.38	1.11
PDF	2.65	2.47	2.21	2.16	1.99	1.90	1.79	1.73	1.50	1.10
ISR	5.23	5.23	5.23	5.23	5.23	5.23	5.23	5.23	5.23	5.23
FSR	5.46	5.46	5.46	5.46	5.46	5.46	5.46	5.46	5.46	5.46
Cross Section	5.00	5.00	5.00	5.00	5.00	5.00	5.00	5.00	5.00	5.00
Z Cross Section	2.78	2.78	2.78	2.78	2.78	2.78	2.78	2.78	2.78	2.78
Luminosity	6.00	6.00	6.00	6.00	6.00	6.00	6.00	6.00	6.00	6.00
Total (%)	11.7	11.6	11.6	11.6	11.5	11.5	11.5	11.5	11.4	11.4

TABLE V: Rate systematic uncertainty (%) for background.

	Fake leptons	Residual photon-conversion	WZ	ZZ
Statistics	2.27	16.90	0.80	3.59
Fake rate	14.08	-	-	-
Residual conversion rate	-	8.84	-	-
MC scale factors	-	-	2.22	2.65
Cross Section	-	-	10.00	10.00
Luminosity	-	-	6.00	6.00
Total (%)	14.3	19.1	11.9	12.5

TABLE VI: Upper limits on the production cross-section times branching fraction $\sigma(p\bar{p}\to Wh) \times B_F(h\to W^{*+}W^{*-})$ at a 95% C.L. as a function of higgs mass.

Higgs Mass (GeV/c^2)	Expected Median (pb)	Observed (pb)
110	$1.54^{+0.64}_{-0.44}$	2.42
120	$1.24^{+0.53}_{-0.34}$	1.80
130	$1.16^{+0.49}_{-0.32}$	1.97
140	$1.05^{+0.44}_{-0.29}$	1.73
150	$1.04^{+0.42}_{-0.29}$	1.82
160	$0.98^{+0.42}_{-0.27}$	1.23
170	$0.97^{+0.40}_{-0.27}$	1.48
180	$0.88^{+0.37}_{-0.24}$	1.23
190	$0.82^{+0.34}_{-0.23}$	1.18
200	$0.76^{+0.31}_{-0.21}$	0.89

TABLE VII: Upper limits on the production cross-section times branching fraction $\sigma(p\bar{p}\to Wh) \times B_F(h\to W^{*+}W^{*-})$ relative to prediction for fermiophobic higgs.

Higgs Mass (GeV/c^2)	Expected Median (Limit/σ_{FH})	Observed (Limit/σ_{FH})
110	$8.2^{+3.4}_{-2.3}$	12.9
120	$8.8^{+3.8}_{-2.4}$	12.9
130	$11.1^{+4.6}_{-3.1}$	18.8
140	$13.0^{+5.5}_{-3.6}$	21.6
150	$16.7^{+6.8}_{-4.7}$	29.4
160	$19.1^{+8.2}_{-5.3}$	23.8
170	$24.0^{+9.8}_{-6.8}$	36.7
180	29^{+12}_{-8}	40.4
190	34^{+14}_{-10}	49.2
200	40^{+17}_{-11}	46.5

TABLE VIII: Upper limits on the production cross-section times branching fraction $\sigma(p\bar{p}\to Wh) \times B_F(h\to W^{*+}W^{*-})$ relative to prediction for SM higgs

Higgs Mass (GeV/c^2)	Expected Median (Limit/σ_{SM})	Observed (Limit/σ_{SM})
110	180^{+74}_{-52}	283.0
120	65^{+28}_{-18}	94.9
130	36^{+15}_{-10}	60.9
140	25^{+11}_{-7}	41.2
150	$22.0^{+8.9}_{-6.2}$	38.7
160	$20.1^{+8.6}_{-5.5}$	25.1
170	$24.0^{+9.8}_{-6.8}$	36.7
180	29^{+12}_{-8}	40.4
190	34^{+14}_{-10}	49.2
200	40^{+17}_{-11}	46.5

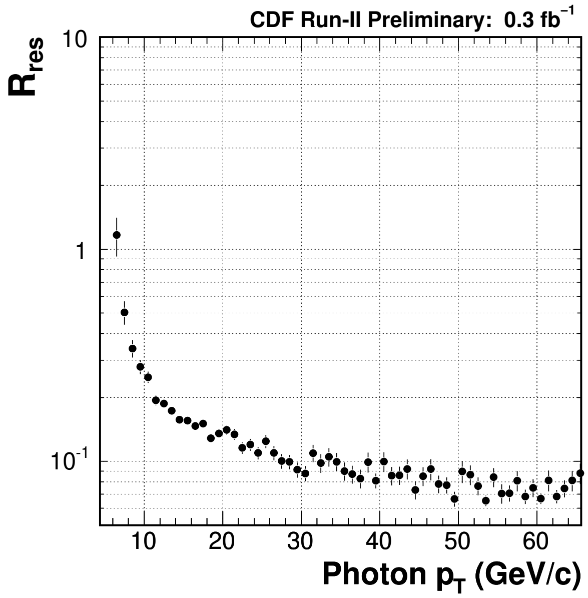

FIG. 1: Residual photon-conversion ratios as a function of photon p_T.

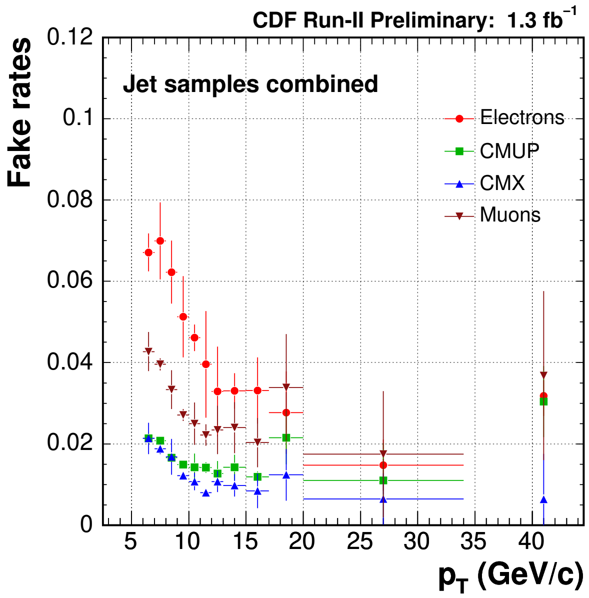

FIG. 2: Fake-lepton rates as a function of isolated track p_T for each lepton object.

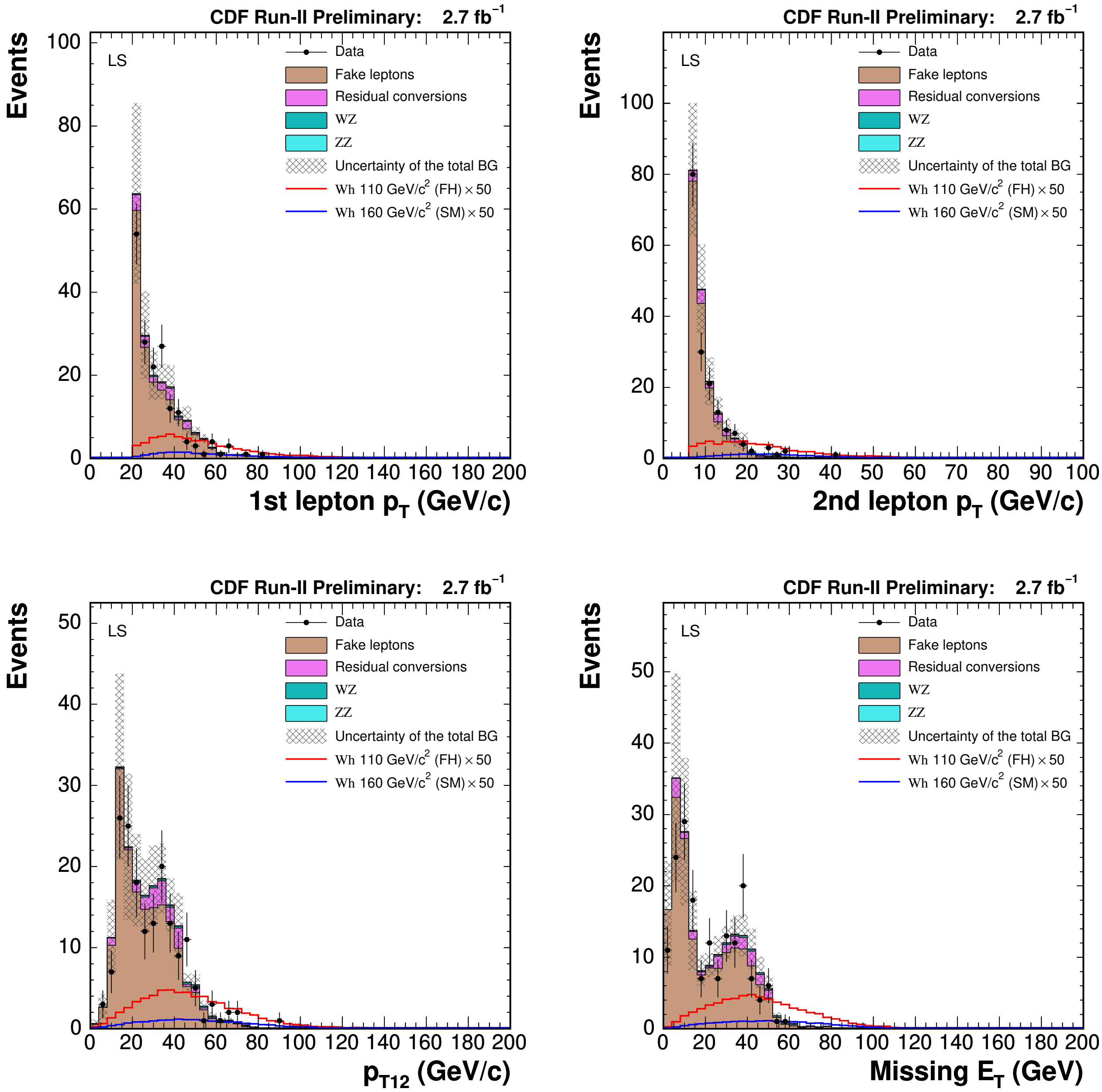

FIG. 3: BDT input variables (1st lepton $p_T(p_{T1})$ and 2nd lepton $p_T(p_{T2})$, Dilepton system $p_T(p_{T12})$, and Missing E_T).

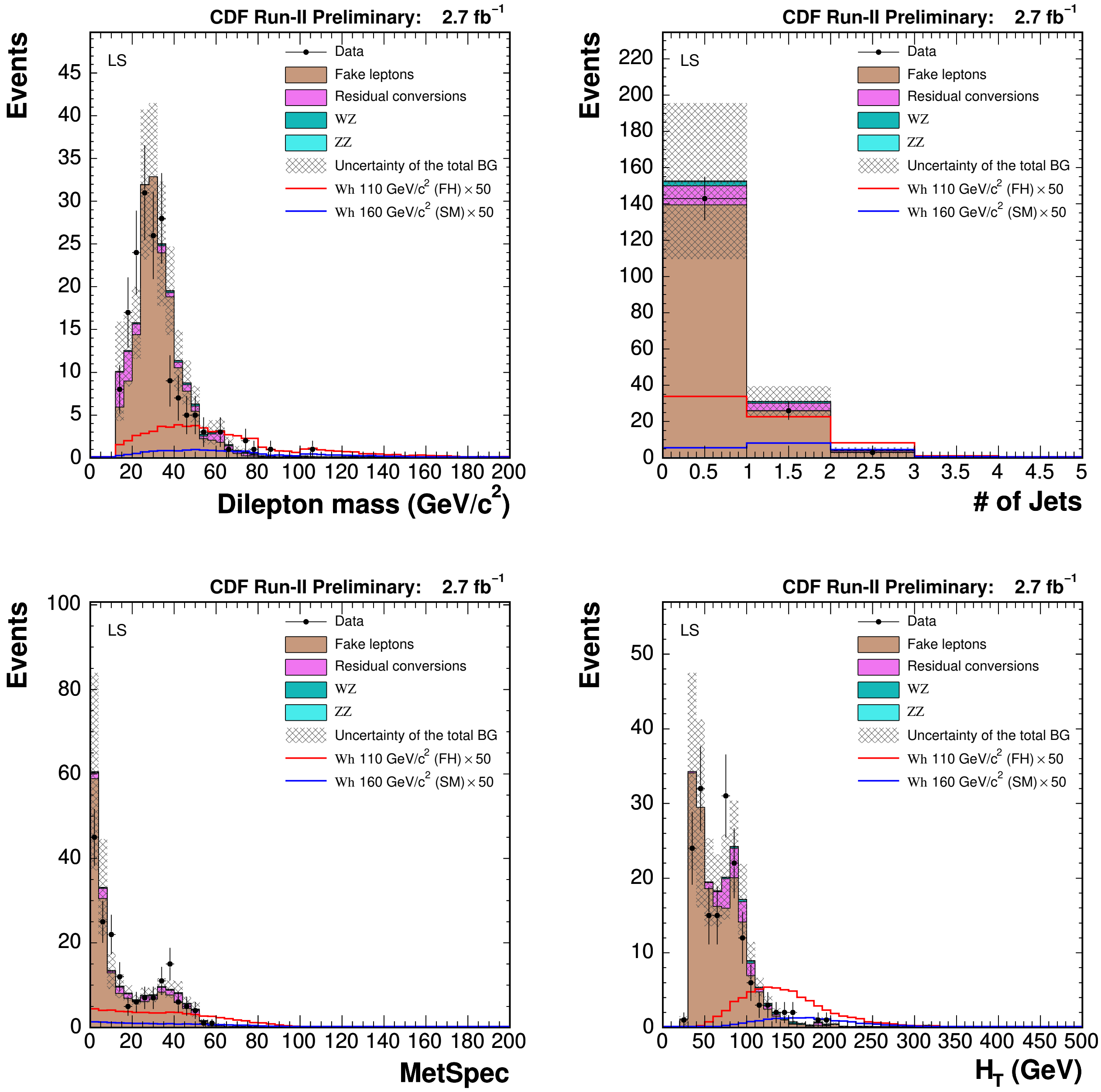

FIG. 4: BDT input variables (Dilepton mass, number of jets, MetSpec, and H_T).

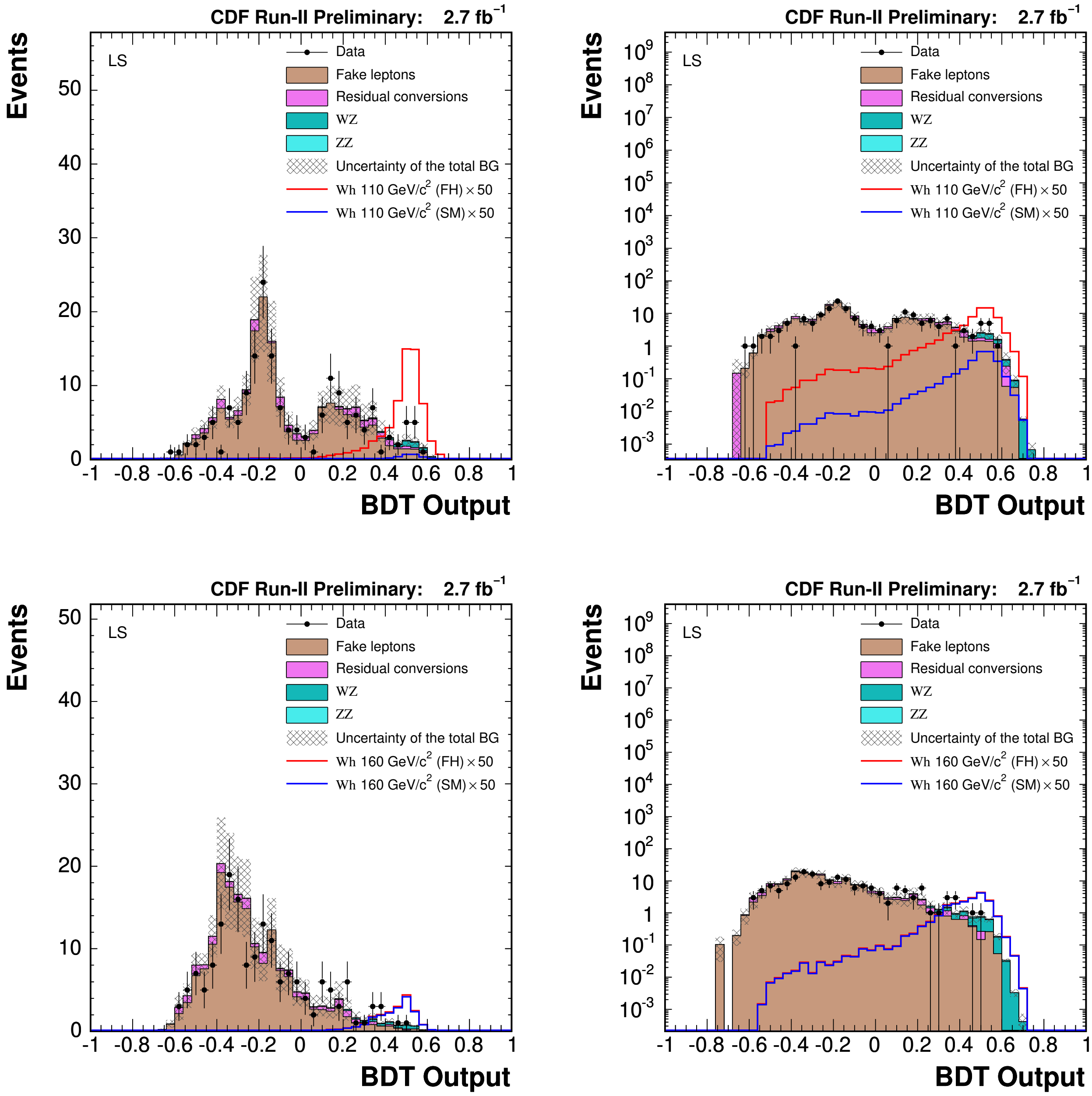

FIG. 5: BDT outputs for $M_h = 110$ and 160 GeV$/c^2$.

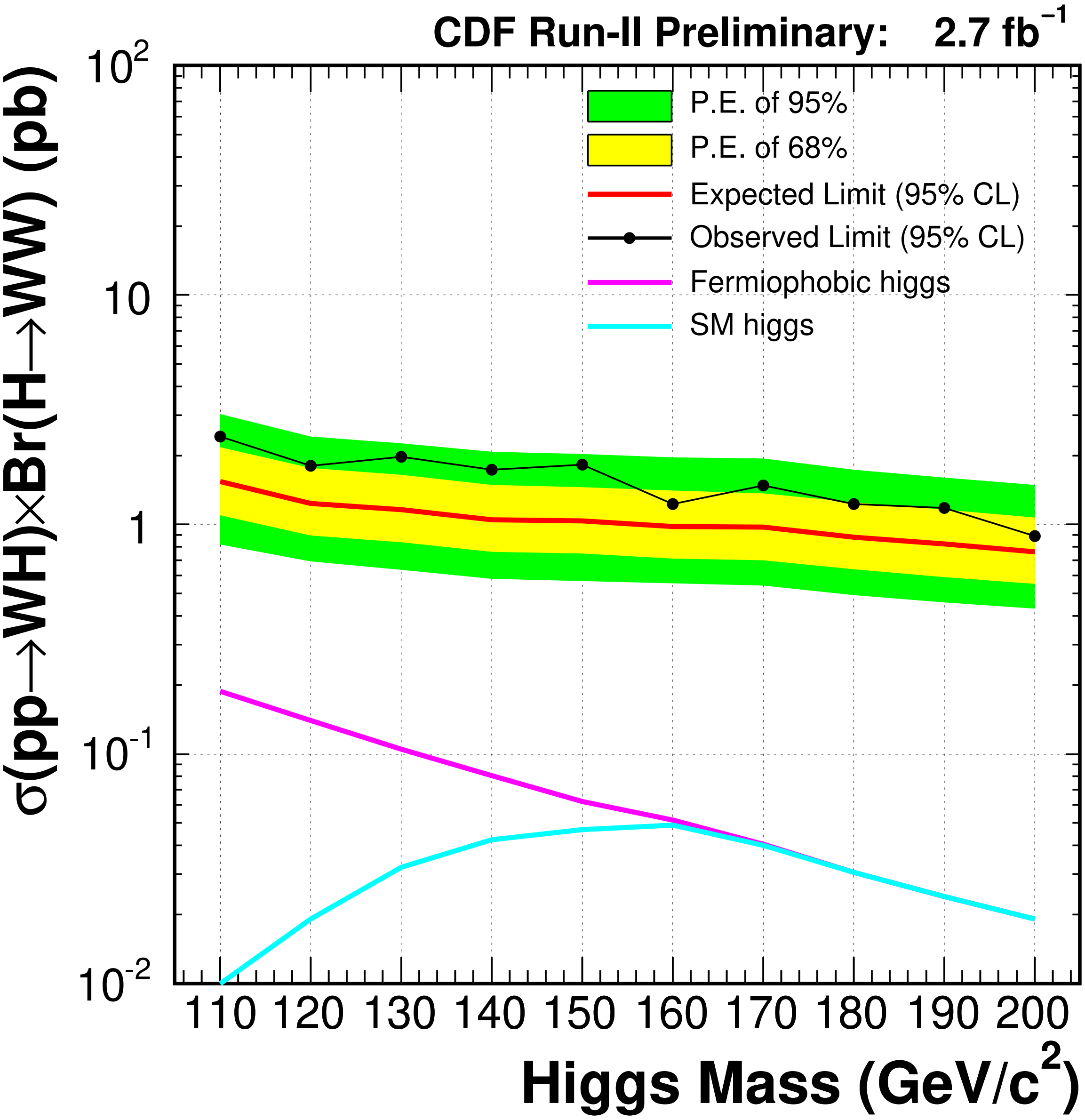

FIG. 6: Upper limits on the production cross-section times branching fraction $\sigma(p\bar{p}\rightarrow Wh) \times B_F(h\rightarrow W^{*+}W^{*-})$ at a 95% C.L. as a function of higgs mass together with the cross sections of the benchmark scenario for the fermiophobic higgs and of the Standard Model.

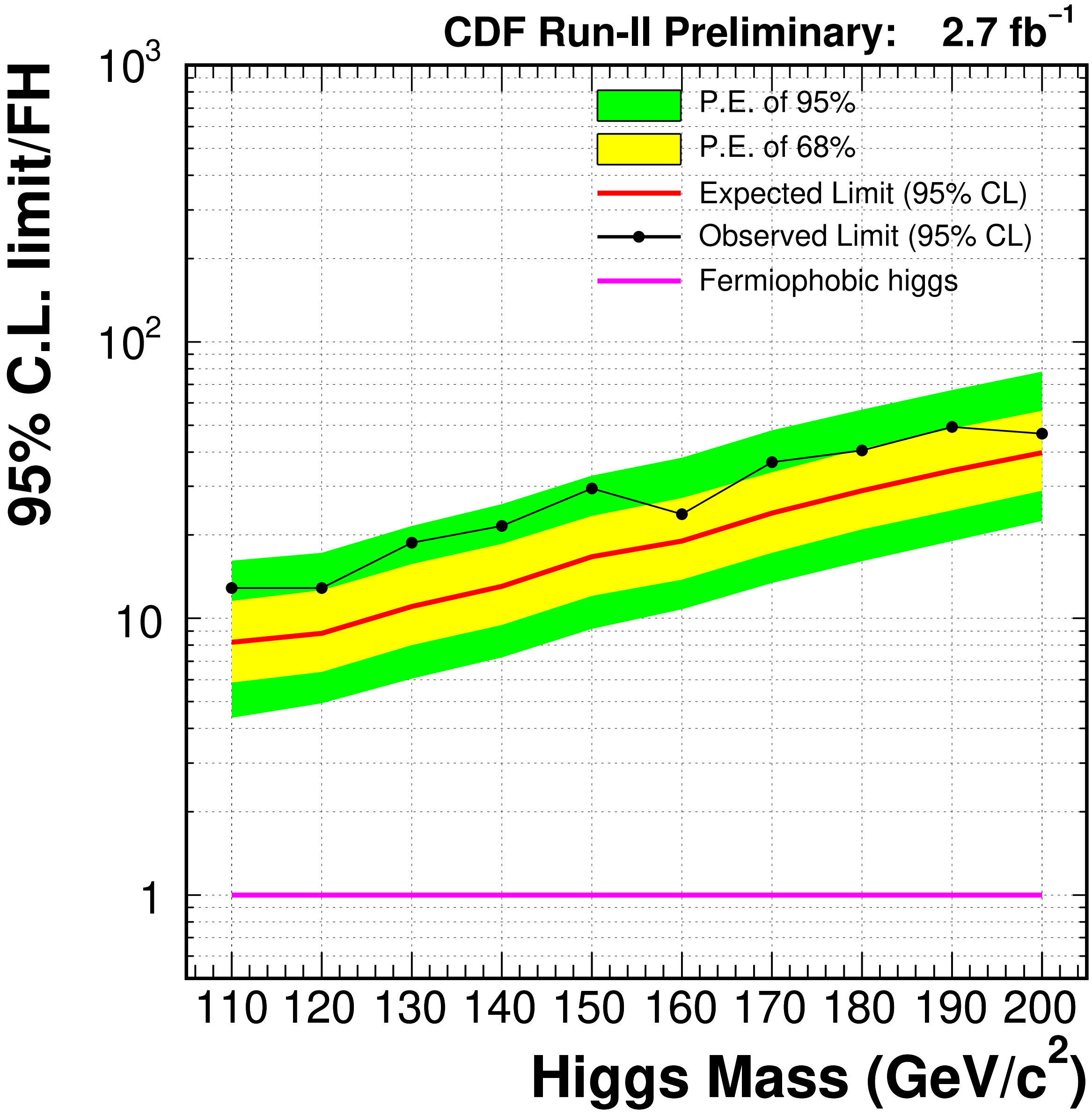

FIG. 7: Upper limits on the production cross-section times branching fraction $\sigma(p\bar{p}\to Wh) \times B_F(h\to W^{*+}W^{*-})$ relative to prediction for fermiophobic higgs at a 95% C.L. as a function of higgs mass.

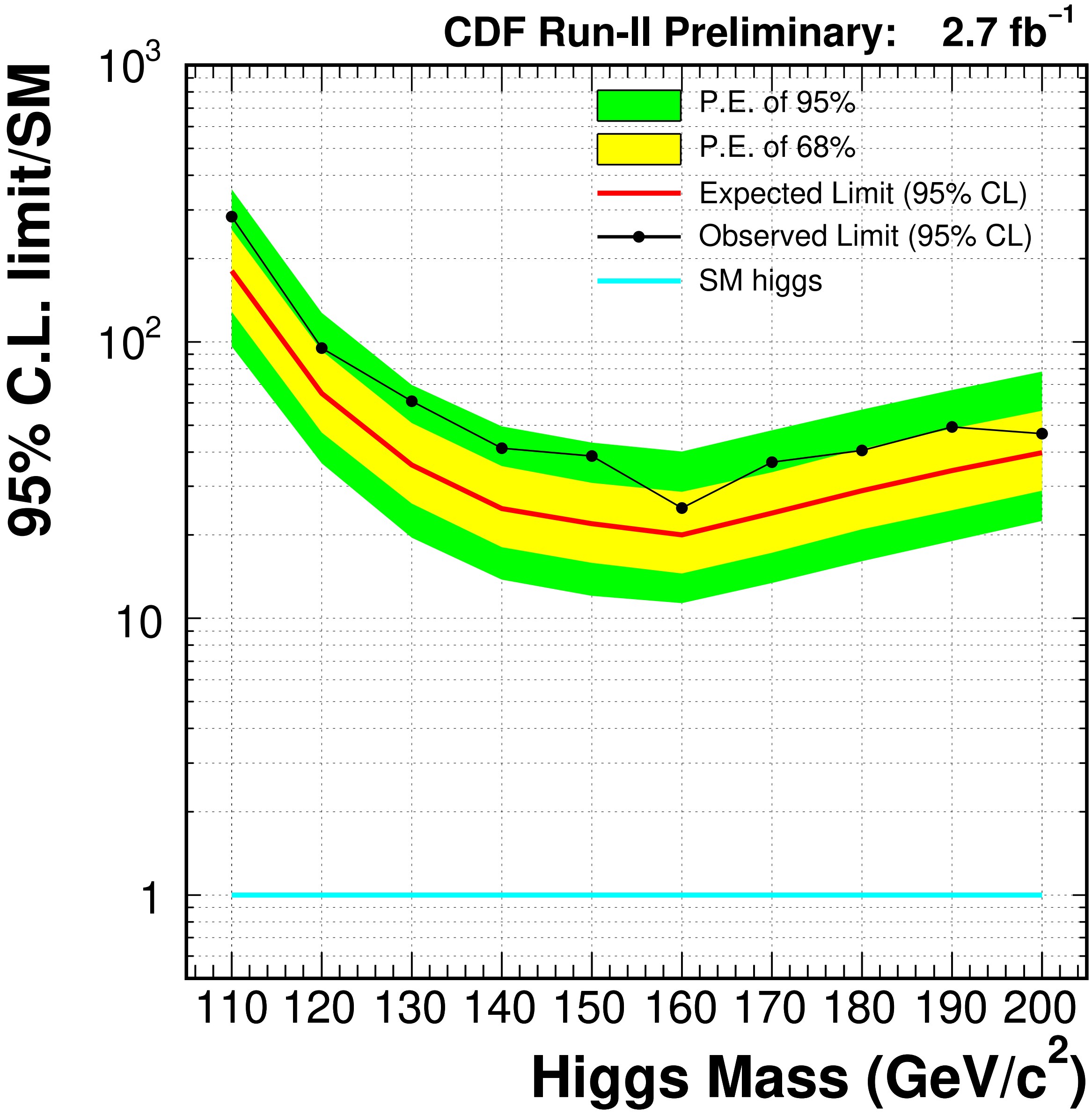

FIG. 8: Upper limits on the production cross-section times branching fraction $\sigma(p\bar{p}\to Wh) \times B_F(h\to W^{*+}W^{*-})$ relative to prediction for SM higgs at a 95% C.L. as a function of higgs mass.

Acknowledgments

We thank the Fermilab staff and the technical staffs of the participating institutions for their vital contributions. This work was supported by the U.S. Department of Energy and National Science Foundation; the Italian Istituto Nazionale di Fisica Nucleare; the Ministry of Education, Culture, Sports, Science and Technology of Japan; the Natural Sciences and Engineering Research Council of Canada; the National Science Council of the Republic of China; the Swiss National Science Foundation; the A.P. Sloan Foundation; the Bundesministerium fuer Bildung und Forschung, Germany; the Korean Science and Engineering Foundation and the Korean Research Foundation; the Particle Physics and Astronomy Research Council and the Royal Society, UK; the Russian Foundation for Basic Research; the Comision Interministerial de Ciencia y Tecnologia, Spain; and in part by the European Community's Human Potential Programme under contract HPRN-CT-20002, Probe for New Physics.

[1] LEP Electroweak Working Group, http://lepwwg.web.cern.ch/LEPEWWG/.
[2] A. Stange, W. Maricano, and S. Willenbrock, Phys. Rev. D **49**, 1354 (1994).
[3] F. Abe, et al., Nucl. Instrum. Methods Phys. Res. A **271**, 387 (1988); D. Amidei, et al., Nucl. Instum. Methods Phys. Res. A **350**, 73 (1994); F. Abe, et al., Phys. Rev. D **52**, 4784 (1995); P. Azzi, et al., Nucl. Instrum. Methods Phys. Res. A **360**, 137 (1995); The CDFII Detector Technical Design Report, Fermilab-Pub-96/390-E
[4] A.Hocker, P.Speckmayer, J.Stelzer, F.Tegenfeldt, H.Voss, K,Voss, "TMVA Toolkit for Multivariate Data Analysis with ROOT Users Guide".